

Chapter 14

Interferometric View of Imaging

The exit pupil of an imaging system contains a Fourier representation of the image. Partial coherence complicates the situation somewhat. A nice way of looking at this is to consider the exit pupil as consisting of a superposition of pairs of pinholes. Each pinhole pair produces a sinusoidal fringe at the image plane with a spatial frequency that depends on the separation of the pinholes. The observed image intensity distribution is composed of the superposition of fringes generated by all possible pairs in the pupil. Since there are many pairs with the same separation, the total amplitude and phase of the spectral component in the intensity, $I_i(v_U, v_V)$ is calculated by adding all of these contributions. The mutual intensity in the exit pupil provides us with a mathematical description of this.

The propagation of mutual intensity from the exit pupil to the image plane is given by:

$$J_i(u_1, v_1; u_2, v_2) = \iiint_{\Sigma_1} \iiint_{\Sigma_1} J_p'(x_1, y_1; x_2, y_2) \exp \left[-j \frac{2\pi}{\lambda} (r_2 - r_1) \right] \frac{\cos \theta_1}{\lambda r_1} \frac{\cos \theta_2}{\lambda r_2} dx_1 dy_1 dx_2 dy_2 \quad (14.1)$$

J_p' represents the mutual intensity emerging from the exit pupil, and J_i is the mutual intensity of the image.

If the distance from the exit pupil to the image is z_i , and further, we define the pupil mutual intensity on the surface a sphere of radius z_i (the “exit sphere”), then after a bit of trigonometry, we can write:

$$J_i(u_1, v_1; u_2, v_2) = \frac{1}{(\lambda z_i)^2} \exp \left\{ j \frac{\pi}{\lambda z_i} [(u_1^2 + v_1^2) - (u_2^2 + v_2^2)] \right\} \quad (14.2)$$

$$\times \iiint_{\Sigma_1} \iiint_{\Sigma_1} J_p'(x_1, y_1; x_2, y_2) \exp \left[-j \frac{2\pi}{\lambda} (x_2 u_2 + y_2 v_2 - x_1 u_1 - y_1 v_1) \right] dx_1 dy_1 dx_2 dy_2$$

and for the image intensity:

$$I_i(u, v) = \frac{1}{(\lambda z_i)^2} \iiint_{\Sigma_1} \iiint_{\Sigma_1} dx_1 dy_1 dx_2 dy_2 J_p'(x_1, y_1; x_2, y_2) \quad (14.3)$$

$$\exp \left\{ -j \frac{2\pi}{\lambda} [(x_2 - x_1)u + (y_2 - y_1)v] \right\}$$

To see the interferometric analogy, let's take the Fourier transform of the image intensity. This tells us how the individual fringe components of the image are constructed:

$$\begin{aligned} \mathcal{I}_i(\mathbf{v}_U, \mathbf{v}_V) = & \frac{1}{(\lambda z_i)^2} \int_{-\infty}^{\infty} \int_{-\infty}^{\infty} \int_{-\infty}^{\infty} dx_1 dy_1 dx_2 dy_2 J_p'(x_1, y_1; x_2, y_2) \\ & \times \int_{-\infty}^{\infty} \int_{-\infty}^{\infty} dU dV \exp \left\{ -j2\pi \left[\left(v_U + \frac{x_2 - x_1}{\lambda z_i} \right) U + \left(v_V + \frac{y_2 - y_1}{\lambda z_i} \right) V \right] \right\} \end{aligned} \quad (14.4)$$

The second double integral is just a delta function with the argument inside the square brackets. We can therefore do the integral over (x_2, y_2) , and we finally obtain:

(14.5)

This relation is telling us that the component of the image spectrum at $(\mathbf{v}_U, \mathbf{v}_V)$ is composed of the integral of all values of the mutual intensity with fixed separation $(\lambda z_i \mathbf{v}_U, \lambda z_i \mathbf{v}_V)$ as the free variables (x_1, y_1) run over the whole pupil plane.

We now relate the result to the mutual intensity incident on the finite exit pupil aperture, J_p :

$$\begin{aligned} \mathcal{I}_i(\mathbf{v}_U, \mathbf{v}_V) = & \int_{-\infty}^{\infty} \int_{-\infty}^{\infty} P(x_1, y_1) P^*(x_1 - \lambda z_i \mathbf{v}_U, y_1 - \lambda z_i \mathbf{v}_V) \\ & \times J_p(x_1, y_1; x_1 - \lambda z_i \mathbf{v}_U, y_1 - \lambda z_i \mathbf{v}_V) dx_1 dy_1 \end{aligned} \quad (14.6)$$

An interesting special case occurs when the object radiates an incoherent field. Then the mutual intensity distribution incident on the “entrance sphere” of radius z_i in the entrance pupil is a function only of the separations $\Delta x, \Delta y$ in that pupil. The quadratic phase factors drop out on the surface of this sphere. The mutual intensity on the exit sphere is then just a magnified version of that on the entrance sphere. Thus J_p is also only a function of coordinate differences, and is independent of x_1, y_1 . We can then write:

$$\mathcal{I}_i(\mathbf{v}_U, \mathbf{v}_V) = J_p(x_1 - \lambda z_i \mathbf{v}_U, y_1 - \lambda z_i \mathbf{v}_V) \int_{-\infty}^{\infty} \int_{-\infty}^{\infty} P(x_1, y_1) P^*(x_1 - \lambda z_i \mathbf{v}_U, y_1 - \lambda z_i \mathbf{v}_V) dx_1 dy_1 \quad (14.7)$$

This equation tells us that for an incoherent object and an aberration free optical system, as the pinhole pair that yields a particular spatial frequency in the image slides around the exit pupil, the phases are identical in all locations. The weighting factor for each spatial frequency component is given simply by the autocorrelation integral, which is none other than the OTF (optical transfer function) for the optical system.


Stellar interferometry

This result suggests that there is a certain redundancy in the imaging system which gives a high signal to noise ratio, but doesn't contribute any extra information. This fact is exploited in stellar interferometers. In one class of such interferometers, it is desired only to determine some rela-

tively simple property of an astronomical object. For example, we may wish to determine only the angular diameter of a circular object. This can be done using only a single pair of pinholes in the pupil plane. The visibility of the fringes observed in the pupil plane is then observed as the pinhole spacing is varied. This directly measures the coherence factor of the light in the exit pupil. A uniform circular incoherent object of radius r_s at distance z from a telescope gives a coherence factor at the entrance pupil of the form:

$$\mu_p(\Delta x, \Delta y) = 2 \left[\frac{J_1\left(\frac{2\pi r_s}{\lambda z} \sqrt{(\Delta x)^2 + (\Delta y)^2}\right)}{\frac{2\pi r_s}{\lambda z} \sqrt{(\Delta x)^2 + (\Delta y)^2}} \right]. \quad (14.8)$$

We define the angular diameter of the object as $\theta_s = 2r_s/z$. Then



(14.9)

So the fringes vanish when the pinhole spacing is at the zero of the Bessel function J_1 . This spacing is given by:



(14.10)

The big advantage of this approach comes with the concept of *aperture synthesis*, which is illustrated in the diagram below of Michelson's stellar interferometer. Here the mirror spacing, s , can be much greater than the physical size of a single practical telescope mirror. Hence the angular diameter of objects that could not otherwise be distinguished from point-like can be determined.

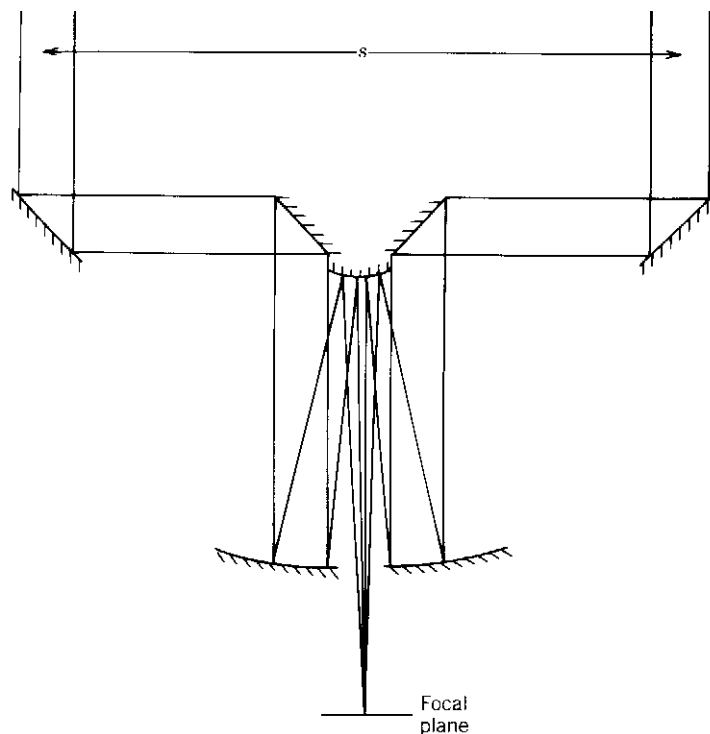


Figure 7-17. Michelson stellar interferometer.

This idea is difficult to implement in the visible, since the pathlengths of the two arms of the interferometer must be maintained to be nearly equal. The tolerance is given by the coherence length of the light being detected. Even worse is that the pathlength difference must be stable to within a fraction of a visible wavelength over the course of the exposure time of the film or detector.

However, the concept of aperture synthesis has enjoyed great success in the radio portion of the spectrum. In a radiotelescope array, the signals from physically separated antennas can be received individually, and interferometrically combined electronically using suitable signal processing electronics. Beyond the simple determination of object size, excellent images can be obtained by constructing arrays of many radiotelescopes. An example array, and a radio image are shown below.

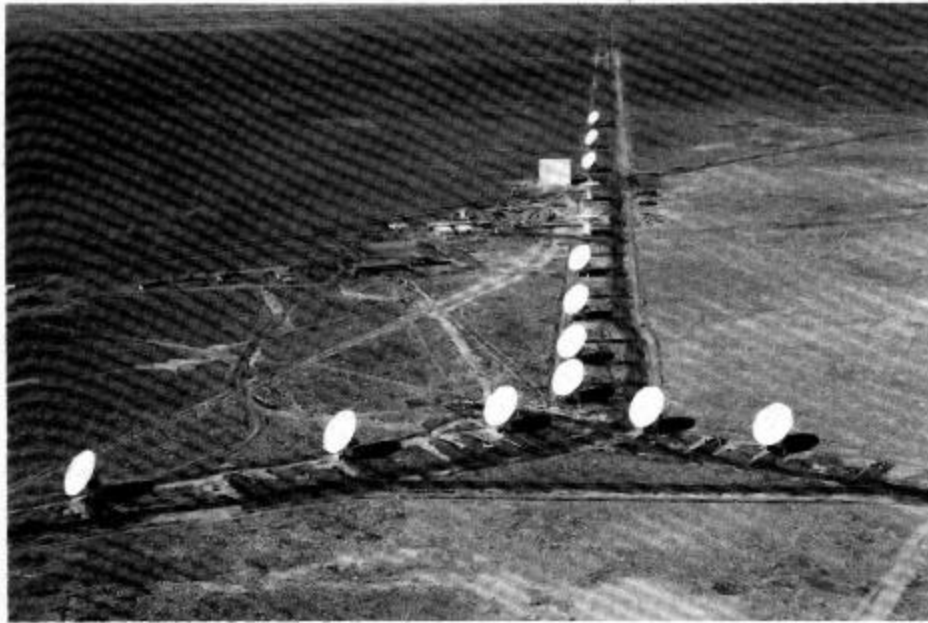


Fig. 6.9. The Very Large Array at Socorro, New Mexico. Aerial view of the VLA looking down the southwest arm; the prominent structure is the Antenna Assembly Building. The north arm branches off to the lower right; the southeast arm extends to the left. The array is shown in its concentrated configuration (courtesy NRAO/AUI)

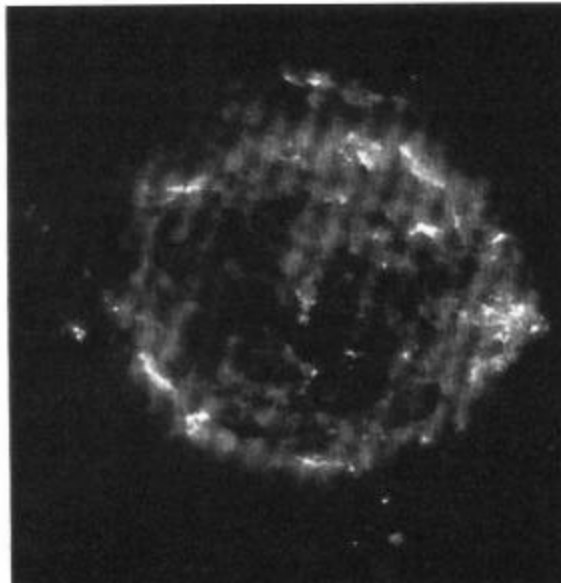


Fig. 9.6. The supernova remnant Cas A from observations with the Cambridge 5 km-radio synthesis telescope (courtesy Mullard Radio Astronomy Observatory)